Inorg. Chem. **2008**, *47*, 3340−3348

Luminescent Cyclometalated Rh^{III}, Ir^{III}, and $(DIP)_2Ru^{II}$ Complexes with Carboxylated Bipyridyl Ligands: Synthesis, X-ray Molecular Structure, and Photophysical Properties

Jenny B. Waern,[†] Christophe Desmarets,[†] Lise-Marie Chamoreau,[†] Hani Amouri,*[,†] Andrea Barbieri,*[,‡] Cristiana Sabatini,[‡] Barbara Ventura,[‡] and Francesco Barigelletti[‡]

Laboratoire de Chimie Inorganique et Matériaux Moléculaires, UMR CNRS 7071, Université Pierre et Marie Curie Paris VI, 4 place Jussieu, case 42, 75252 Paris Cedex 05, France, and Istituto per la Sintesi Organica e la Fotoreattività (ISOF), Consiglio Nazionale delle Ricerche (CNR), Via P. Gobetti 101, 40129 Bologna, Italy

Received November 27, 2007

Luminescent cyclometalated rhodium(III) and iridium(III) complexes of the general formula $[M(ppy)_2(N^\wedge N)][PF_6]$, with N^N = Hcmbpy = 4-carboxy-4′-methyl-2,2′-bipyridine and M = Rh (**1**), Ir (**2**) and N^N = H_2dcbpy = 4,4′-dicarboxy-2,2′-bipyridine and M = Rh (**3**), Ir (**4**), were prepared in high yields and fully characterized. The X-ray molecular structure of the monocarboxylic iridium complex $[Ir(ppy)_2(Hcmbpy)][PF_6]$ (**2**) was also determined. The photophysical properties of these compounds were studied and showed that the photoluminescence of rhodium complexes **1** and **3** and iridium complexes **2** and **4** originates from intraligand charge-transfer (ILCT) and metal-to-ligand charge-transfer/ligand-centered MLCT/LC excited states, respectively. For comparison purposes, the *mono*- and *di*carboxylic acid ruthenium complexes $[Ru(DIP)_2(Hcmbpy)][Cl]_2$ (**5**) and $[Ru(DIP)_2(H_2dcbpy)][Cl]_2$ (**6**), where DIP = 4,7-diphenyl-1,10-phenanthroline, were also prepared, whose emission is MLCT in nature. Comparison of the photophysical behavior of these rhodium(III), iridium(III), and ruthenium(II) complexes reveals the influence of the carboxylic groups that affect in different ways the ILCT, MLCT, and LC states.

Introduction

The design of luminescent inorganic materials based on transition-metal complexes has long been under intense investigation in academic and industrial laboratories.[1–5] In particular, iridium cyclometalated complexes have attracted significant interest because of their remarkable photoluminescent properties[6] and have shown to be amenable to important applications, among others as active components in organic light-emitting diodes,[7–9] and single-layer emitting diodes,[4,10–13] unimolecular oxygen sensors[14–16]> and as biological labeling reagents.[17–22] These d^6 complexes are attractive in photochemical applications because they generally have long-lived emitting states and high luminescence efficiencies; for example, for *fac*-$Ir(ppy)_3$ (ppy = 2-phenylpyridine), $\phi_{em} = 0.4$ in fluid solutions.[23] Among others, these properties are due to efficient intersystem crossing between the singlet and triplet excited states brought about the strong spin–orbit coupling of the iridium(III) metal ion (coupling constant, $\zeta_{Ir} = 3909\ cm^{-1}$).[24] These complexes, together with their rhodium(III) homologues, are widely studied,[6,25] and the incorporation of various functional groups onto either the cyclometalating ligands (e.g., 2-phenylpyri-

* To whom correspondence should be addressed. E-mail: amouri@ccr.jussieu.fr (H.A.), and barbieri@isof.cnr.it (A.B.).
† Université Pierre et Marie Curie Paris VI.
‡ Istituto ISOF-CNR.

(1) Kalyanasundaram, K. *Photochemistry of Polypyridine and Porphyrin Complexes*; Academic Press: London, U.K., 1992.
(2) Balzani, V.; Scandola, F. *Supramolecular Photochemistry*; Ellis Horwood: New York, 1991.
(3) Balzani, V.; Venturi, M.; Credi, A. *Molecular Devices and Machines: A Journey into the Nanoworld*; Wiley-VCH: Weinheim, Germany, 2003.
(4) Holder, E.; Langeveld, B. M. W.; Schubert, U. S. *Adv. Mater.* **2005**, *17*, 1109–1121.
(5) Coe, B. J.; Curati, N. R. M. *Comments Inorg. Chem.* **2004**, *25*, 147–184.
(6) Flamigni, L.; Barbieri, A.; Sabatini, C.; Ventura, B.; Barigelletti, F. *Top. Curr. Chem.* **2007**, *281*, 143–203.
(7) Baldo, M. A.; Lamansky, S.; Burrows, P. E.; Thompson, M. E.; Forrest, S. R. *Appl. Phys. Lett.* **1999**, *75*, 4–6.
(8) Adachi, C.; Baldo, M. A.; Forrest, S. R.; Lamansky, S.; Thompson, M. E.; Kwong, R. C. *Appl. Phys. Lett.* **2001**, *78*, 1622–1624.
(9) Adachi, C.; Baldo, M. A.; Forrest, S. R.; Thompson, M. E. *Appl. Phys. Lett.* **2000**, *77*, 904–906.

10.1021/ic702327z CCC: $40.75
Published on Web 03/15/2008

dine) or the polypyridyl ligands (e.g., bipyridine) in heteroleptic complexes of the kind $[Ir(ppy)_2(N^\wedge N)]^+$ can be readily achieved.[26–28] In particular, extensive studies have shown that the variation of the functional groups in the complexes allows fine-tuning of the emission color with changes ranging from green to blue[29] and to red.[30] On the other hand, polypyridine ligands with carboxylate moieties have been used as building blocks for a variety of supramolecular assemblies[31–33] and also represent a suitable functionalization for the anchoring to a semiconductor surface in dye-sensitized photoelectrochemical solar cells.[34,35] Despite being of interest for fundamental studies and technological applications, transition-metal complexes with ligands bearing carboxylate groups have not been investigated to a large extent because of the presence of acid/base equilibria, which complicates the interpretation of their photophysical behavior.

In this paper, we report the synthesis of new cyclometalated rhodium(III) and iridium(III) complexes incorporating carboxylated bipyridine ligands of the general formula $[M(ppy)_2(N^\wedge N)][PF_6]$ with N^N = Hcmbpy = 4-carboxy-4′-methyl-2,2′-bipyridine and M = Rh (**1**), Ir (**2**) and N^N = H_2dcbpy = 4,4′-dicarboxy-2,2′-bipyridine and M = Rh (**3**), Ir (**4**). For comparison purposes, the *mono*- and *di*carboxylic acid ruthenium complexes $[Ru(DIP)_2(Hcmbpy)][Cl]_2$ (**5**) and $[Ru(DIP)_2(H_2dcbpy)][Cl]_2$ (**6**) were prepared and their photophysical properties are presented (DIP = 4,7-diphenyl-1,10-phenanthroline). In these complexes, color tuning of luminescence is achieved via the electron-withdrawing effect of the carboxylate groups, which influences to different degrees the energy levels of intraligand charge-transfer (ILCT), metal-to-ligand charge-transfer (MLCT), and ligand-centered (LC, π,π^*) states. The X-ray molecular structure of the monocarboxylic iridium complex $[Ir(ppy)_2(Hcmbpy)][PF_6]$ (**2**) was also determined.

Scheme 1

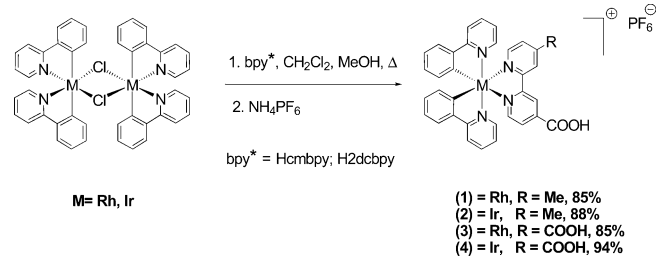

Results and Discussion

Synthesis and Characterization of $[M(ppy)_2(Hcmbpy)][PF_6]$ [M = Rh (1), Ir (2)] and $[M(ppy)_2(H_2dcbpy)][PF_6]$ [M = Rh (3), Ir (4)]. The dichloro-bridged orthometalated phenylpyridine dimers $[M(ppy)_2(\mu\text{-Cl})]_2$ with M = Rh, Ir were prepared according to literature procedures.[30,36,37] As for the monocarboxylic rhodium complex $[Rh(ppy)_2(Hcmbpy)][PF_6]$ (**1**) and the dicarboxylated derivative $[Rh(ppy)_2(H_2dcbpy)][PF_6]$ (**3**), they were prepared according to an experimental procedure developed in our laboratory. Thus, treatment of $[Rh(ppy)_2(\mu\text{-Cl})]_2$ with the appropriate carboxylated bpy ligands (see Scheme 1) in a CH_2Cl_2/MeOH solution at reflux produced an orange-yellow solution, and subsequent addition of a saturated methanol solution of NH_4PF_6 provided the pure complexes as precipitates of hexafluorophosphate salts. In a similar way, the iridium series $[Ir(ppy)_2(Hcmbpy)][PF_6]$ (**2**) or $[Ir(ppy)_2(H_2dcbpy)][PF_6]$ (**4**) were prepared. Although complexes such as $[Ir(ppy)_2(L_2)]^+$, where L_2 is a functionalized polypyridyl ligand, are well-known, in contrast those featuring carboxylated bpy ligands were less investigated.[38–40]

(10) Slinker, J. D.; Gorodetsky, A. A.; Lowry, M. S.; Wang, J. J.; Parker, S.; Rohl, R.; Bernhard, S.; Malliaras, G. G. *J. Am. Chem. Soc.* **2004**, *126*, 2763–2767.
(11) Lamansky, S.; Djurovich, P. I.; Abdel-Razzaq, F.; Garon, S.; Murphy, D. L.; Thompson, M. E. *J. Appl. Phys.* **2002**, *92*, 1570–1575.
(12) Markham, J. P. J.; Lo, S. C.; Magennis, S. W.; Burn, P. L.; Samuel, I. D. W. *Appl. Phys. Lett.* **2002**, *80*, 2645–2647.
(13) Ostrowski, J. C.; Robinson, M. R.; Heeger, A. J.; Bazan, G. C. *Chem. Commun.* **2002**, 784–785.
(14) DeRosa, M. C.; Mosher, P. J.; Yap, G. P. A.; Focsaneanu, K. S.; Crutchley, R. J.; Evans, C. E. B. *Inorg. Chem.* **2003**, *42*, 4864–4872.
(15) Amao, Y.; Ishikawa, Y.; Okura, I. *Anal. Chim. Acta* **2001**, *445*, 177–182.
(16) DiMarco, G.; Lanza, M.; Pieruccini, M.; Campagna, S. *Adv. Mater.* **1996**, *8*, 576–&.
(17) Lo, K. K. W.; Chan, J. S. W.; Lui, L. H.; Chung, C. K. *Organometallics* **2004**, *23*, 3108–3116.
(18) Lo, K. K. W.; Chung, C. K.; Lee, T. K. M.; Lui, L. H.; Tsang, K. H. K.; Zhu, N. Y. *Inorg. Chem.* **2003**, *42*, 6886–6897.
(19) Lo, K. K. W.; Hui, W. K.; Chung, C. K.; Tsang, K. H. K.; Lee, T. K. M.; Li, C. K.; Lau, J. S. Y.; Ng, D. C. M. *Coord. Chem. Rev.* **2006**, *250*, 1724–1736.
(20) Lo, K. K. W.; Lau, J. S. Y. *Inorg. Chem.* **2007**, *46*, 700–709.
(21) Lo, K. K. W.; Li, C. K.; Lau, J. S. Y. *Organometallics* **2005**, *24*, 4594–4601.
(22) Lo, K. K. W.; Ng, D. C. M.; Chung, C. K. *Organometallics* **2001**, *20*, 4999–5001.
(23) King, K. A.; Spellane, P. J.; Watts, R. J. *J. Am. Chem. Soc.* **1985**, *107*, 1431–1432.
(24) Montalti, M.; Credi, A.; Prodi, L.; Gandolfi, M. T. *Handbook of Photochemistry*; CRC Press: Boca Raton, FL, 2006.
(25) Indelli, M. T.; Chiorboli, C.; Scandola, F. *Top. Curr. Chem.* **2007**, *280*, 215–255.
(26) Lamansky, S.; Djurovich, P.; Murphy, D.; Abdel-Razzaq, F.; Kwong, R.; Tsyba, I.; Bortz, M.; Mui, B.; Bau, R.; Thompson, M. E. *Inorg. Chem.* **2001**, *40*, 1704–1711.
(27) Lamansky, S.; Djurovich, P.; Murphy, D.; Abdel-Razzaq, F.; Lee, H. E.; Adachi, C.; Burrows, P. E.; Forrest, S. R.; Thompson, M. E. *J. Am. Chem. Soc.* **2001**, *123*, 4304–4312.
(28) Tsuboyama, A.; Iwawaki, H.; Furugori, M.; Mukaide, T.; Kamatani, J.; Igawa, S.; Moriyama, T.; Miura, S.; Takiguchi, T.; Okada, S.; Hoshino, M.; Ueno, K. *J. Am. Chem. Soc.* **2003**, *125*, 12971–12979.
(29) Sajoto, T.; Djurovich, P. I.; Tamayo, A.; Yousufuddin, M.; Bau, R.; Thompson, M. E.; Holmes, R. J.; Forrest, S. R. *Inorg. Chem.* **2005**, *44*, 7992–8003.
(30) Nonoyam, M. *Bull. Chem. Soc. Jpn.* **1974**, *47*, 767–768.
(31) Cooke, M. W.; Hanan, G. S.; Loiseau, F.; Campagna, S.; Watanabe, M.; Tanaka, Y. *Angew. Chem., Int. Ed.* **2005**, *44*, 4881–4884.
(32) Coppo, P.; Duati, M.; Kozhevnikov, V. N.; Hofstraat, J. W.; De Cola, L. *Angew. Chem., Int. Ed.* **2005**, *44*, 1806–1810.
(33) Cotton, F. A.; Lin, C.; Murillo, C. A. *Acc. Chem. Res.* **2001**, *34*, 759–771.
(34) Campagna, S.; Puntoriero, F.; Nastasi, F.; Bergamini, G.; Balzani, V. *Top. Curr. Chem.* **2007**, *280*, 117–214.
(35) Gratzel, M. *J. Photochem. Photobiol. A: Chem.* **2004**, *164*, 3–14.
(36) Sprouse, S.; King, K. A.; Spellane, P. J.; Watts, R. J. *J. Am. Chem. Soc.* **1984**, *106*, 6647–6653.
(37) Rasmussen, S. C.; Richter, M. M.; Yi, E.; Place, H.; Brewer, K. J. *Inorg. Chem.* **1990**, *29*, 3926–3932.
(38) Caspar, R.; Amouri, H.; Gruselle, M.; Cordier, C.; Malezieux, B.; Duval, R.; Leveque, H. *Eur. J. Inorg. Chem.* **2003**, 499–505.
(39) Caspar, R.; Musatkina, L.; Tatosyn, A.; Amouri, H.; Gruselle, M.; Guyard-Duhayon, C.; Duval, R.; Cordier, C. *Inorg. Chem.* **2004**, *43*, 7986–7993.
(40) Caspar, R.; Cordier, C.; Waern, J. B.; Guyard-Duhayon, C.; Gruselle, M.; Le Floch, P.; Amouri, H. *Inorg. Chem.* **2006**, *45*, 4071–4078.

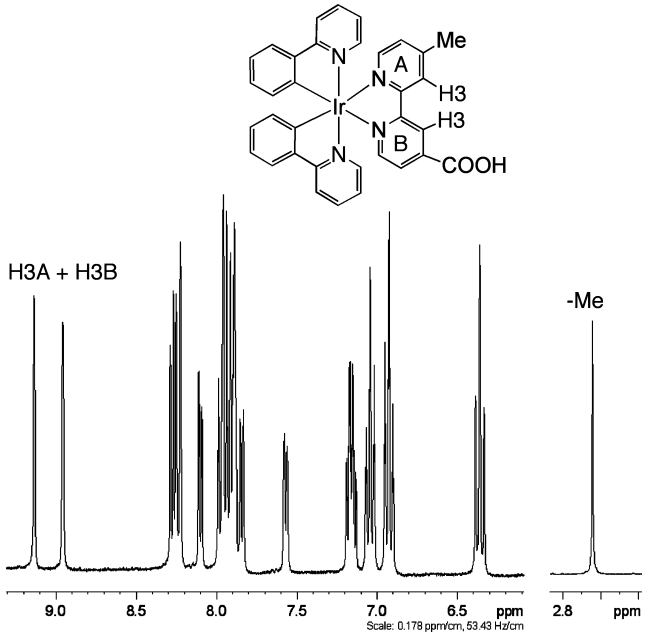

Figure 1. ^{1}H NMR spectrum (300 MHz) of **2** in $(CD_3)_2CO$.

The ^{1}H NMR spectra of the dicarboxylated rhodium and iridium complexes **3** and **4** recorded in acetone-d_6 showed the presence of 11 multiplets, as expected for complexes with C_2 symmetry.[41] For instance, the proton signals H3 and H3′ adjacent to the COOH functions appeared as a singlet and downfield at δ 9.30 for the rhodium complex **3** and at δ 9.33 for the iridium congener **4**. The monocarboxylated compounds **1** and **2**, however, displayed a more complicated NMR spectral pattern due to lack of symmetry (see Figure 1).

For instance, two signals were observed to the protons H3A and H3B adjacent to the carboxylic and to the methyl groups. These signals appeared downfield at 8.78 and 9.07 ppm for the rhodium complex **1** and at 8.94 and 9.12 ppm for the iridium congener **2**. Further, a singlet for the methyl group was observed at δ 3.33 ppm for **1** and at δ 2.64 ppm for **2**. The ^{13}C NMR data of the above complexes were also determined and confirmed the formation of the desired compounds. Elemental analysis also suggested the formation of the above compounds (see the Experimental Section). Furthermore, the X-ray molecular structure of monocarboxylic iridium complex **2** was determined.

X-ray Molecular Structure of 2. Suitable crystals of the monocarboxylated iridium complex were obtained by slow evaporation of Et_2O into an CH_2Cl_2 solution of **2**. Crystallographic data for **2** are shown in Table 1. Complex **2** crystallizes in the monoclinic unit cell with space group $P2_1/n$. A view of the cationic part with atom labeling and selected bond distances and angles is shown in Figure 2. The Ir^{III} center adopts an octahedral geometry with cis-metalated C atoms and trans N atoms, as revealed by previous structural studies on mononuclear species containing (ppy) cyclometalated bidentate ligands.[18,42,43] The Ir−N bond distances

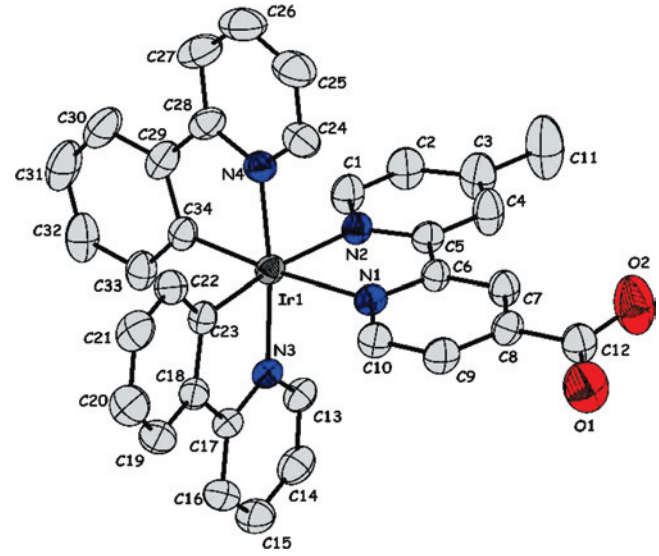

Figure 2. View of the cationic part of **2** [C = gray, O = red, N = blue; H atoms are omitted). The thermal ellipsoids correspond to 50% probability. Selected bond lengths (Å) and angles (deg): Ir1−N1 = 2.151(4), Ir1−N2 = 2.154(3), Ir1−N3 = 2.057(4), Ir1−N4 = 2.061(4), Ir1−C23 = 2.020(4), Ir1−C34 = 2.019(4); C34−Ir1−C23 = 92.25(17), N1−Ir1−N2 = 76.44(13), N4−Ir1−N2 = 87.90(14), N4−Ir1−N1 = 97.15(15), C34−Ir1−N4 = 80.36(18), C23−Ir1−N4 = 95.24(17), N3−Ir1−N4 = 173.65(14).

Table 1. Crystal Data and Structure Refinement for **2**

complex	**2**
formula	$C_{38}H_{36}O_3N_4Ir(PF_6)$
fw	933.88
space group	$P2_1/n$
a (Å)	16.139(2)
b (Å)	13.6478(14)
c (Å)	17.6583(14)
α (deg)	
β (deg)	101.651(8)
γ (deg)	
V (Å^3)	3809.3(7)
Z	4
ρ_{calcd} (g cm^{-3})	1.628
temp (K)	250(2)
λ(Mo Kα) (Å)	0.71073
μ (mm^{-1})	3.618
$R(F_o)^a$	0.0396
wR_2^b	0.0973

^{a} $R = [\sum(|F_o| - |F_c|)/\sum F_o$. ^{b} $wR_2 = \{\sum[w(F_o^2 - F_c^2)^2]/\sum[w(F_o^2)^2]\}^{1/2}$.

in the pyridyl moiety of the two chelating C^N ligands are about ∼2.06 Å, while those of the phenyl ring Ir−C are about ∼2.02 Å. The Ir−N bond distance of the chelating N^N ligand (2.15 Å) is longer than that of Ir−N (C^N) because of the trans influence of the C donor in (ppy). Further analysis of the structure of **2** shows the presence of hydrogen bonding between the carboxylic group (−COOH) and the F atom of $[PF_6]^-$ anion.

Photophysical Properties of $[M(ppy)_2(N^N)][PF_6]$ [M = Rh, Ir (1–4)] and $[Ru(DIP)_2(N^N)][Cl]_2$ (5 and 6) Complexes. Absorption. Absorption spectra recorded in acetonitrile solutions for the four cyclometalated rhodium and iridium complexes (**1–4**) are shown in Figure 3 (top), while the spectra for the two $[Ru(DIP)_2(N^N)]^{2+}$ (**5** and **6**) derivatives are shown in Figure 3 (bottom). Concerned data

(41) Garces, F. O.; Watts, R. J. *Magn. Reson. Chem.* **1993**, *31*, 529–536.
(42) Neve, F.; La Deda, M.; Crispini, A.; Bellusci, A.; Puntoriero, F.; Campagna, S. *Organometallics* **2004**, *23*, 5856–5863.
(43) Zhao, Q.; Liu, S. J.; Shi, M.; Wang, C. M.; Yu, M. X.; Li, L.; Li, F. Y.; Yi, T.; Huang, C. H. *Inorg. Chem.* **2006**, *45*, 6152–6160.

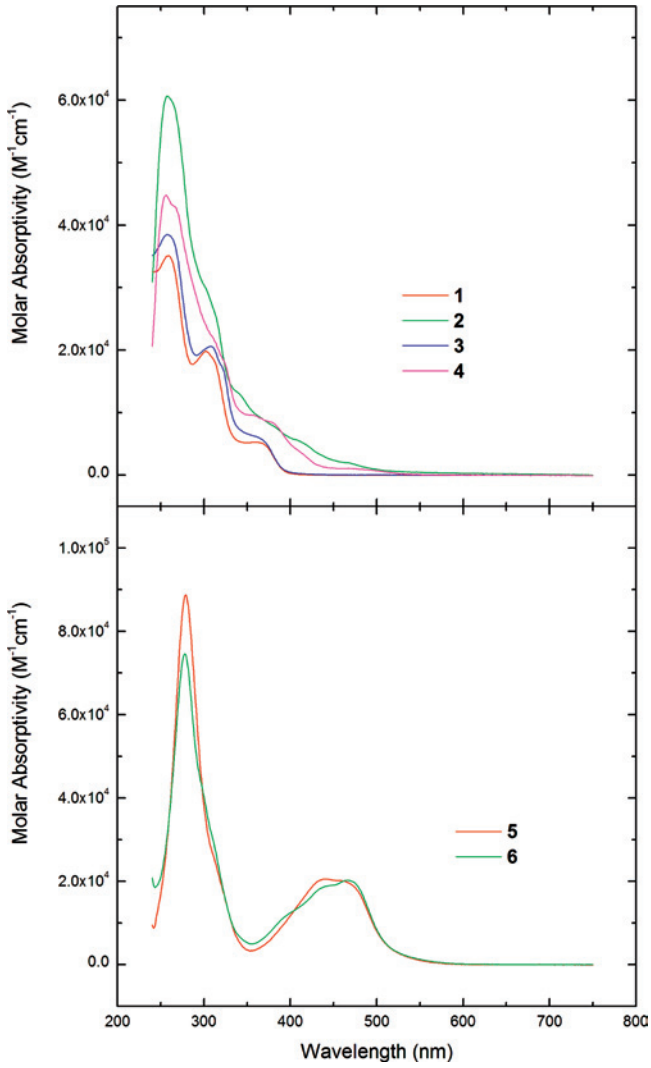

Figure 3. Ground-state absorption spectra for the complexes in a CH_3CN solution. Top panel: [Rh(ppy)$_2$(Hcmbpy)][PF$_6$] (**1**, red line), [Ir(ppy)$_2$(Hcmbpy)][PF$_6$] (**2**, green line), [Rh(ppy)$_2$(H$_2$dcbpy)][PF$_6$] (**3**, blue line), and [Ir(ppy)$_2$(H$_2$dcbpy)][PF$_6$] (**4**, magenta line). Bottom panel: [Ru(DIP)$_2$(Hcmbpy)][Cl]$_2$ (**5**, red line) and [Ru(DIP)$_2$(H$_2$dcbpy)][Cl] (**6**, green line).

are collected in Table 2, together with luminescence results to be discussed below.

In the high-energy region, the absorption profiles of the investigated rhodium(III) and iridium(III) complexes show a similar envelope of electronic transition (Figure 3, top). The intense bands with extinction coefficient $\epsilon > 35\,000$ M^{-1} cm^{-1}, appearing around 260 and 310–320 nm, are assigned to spin-allowed ligand-centered transitions ^{1}LC ($^1\pi,\pi^*$) localized at the ppy and bpy ligands. For these complexes, the low intensity of the bands showing up at lower energy ($\epsilon < 10\,000$ M^{-1} cm^{-1}, in the range $360 < \lambda < 500$ nm) is not compatible with $^1\pi,\pi^*$ allowed transitions. Notably, it is known that the rhodium(III) cyclometalated complexes are quite difficult to oxidize, whereas oxidation processes are more easily observed for the analogous iridium(III) cases.[25,44,45] In organometallic compounds, a large degree of covalency in the metal−C$^-$ σ bonds exists. Then, a simple assumption frequently used to interpret the spectroscopic properties of inorganic complexes, i.e., that both the ground and excited states can be described by a localized molecular orbital configuration,[46] is less applicable. On these bases, for the studied rhodium(III) complexes, it seems reasonable to ascribe the low-intensity absorption features in the range $360 < \lambda < 400$ nm (see Figure 3) to ^{1}SBLCT transitions (σ-bond-to-ligand charge transfer).[25,44,45] With regard to the iridium(III) species, transitions with a mixed ^{1}MLCT/^{1}ILCT character are likely to contribute.[47] In addition, the long tail present in the spectra of the iridium complexes extending in the region of $\lambda > 400$ nm, and (on the contrary) absent in the corresponding rhodium derivatives, is likely to include singlet-to-triplet transitions of spin-forbidden character. This would be a consequence of the heavy-atom effect, owing to the more than 3-fold greater spin–orbit coupling constant of iridium with respect to that of rhodium ($\zeta_{Ir} = 3909$ cm^{-1} and $\zeta_{Rh} = 1259$ cm^{-1}).[24] For the rhodium and iridium derivatives investigated, there is no evident effect on the energy and intensity of the absorption bands of the substituents attached to the ancillary bpy ligand.

As far as the ruthenium derivatives are concerned (Figure 3, bottom), they show the characteristic intense and narrow ^{1}LC ($^1\pi,\pi^*$ bpy-centered) transition, localized in the UV region around 280 nm ($\epsilon \sim 80\,000$ M^{-1} cm^{-1}).[1,46,48] Even in the case of the ruthenium(II) complexes, the energy and intensity of this band does not seem to be affected by the substituents attached to the 4,4′ positions of the pyridine rings. The ^{1}LC transitions of the phenanthroline moiety are somehow merged with those of the bpy band and appear as a shoulder around 310 nm ($\epsilon \sim 30\,000$ M^{-1} cm^{-1}). The visible region of the spectrum is dominated by the ^{1}MLCT transition typical of the ruthenium(II) polypyridyl systems ($400 < \lambda < 520$ nm, $\epsilon \sim 20\,000$ M^{-1} cm^{-1}).[48] For a discussion on the carboxylate/carboxylic acid equilibrium, see below.

Luminescence. All complexes were found to luminesce in air-equilibrated and deoxygenated acetonitrile solutions at room temperature. The luminescence results obtained are gathered in Table 2, together with the results for [Ru(bpy)$_3$]$^{2+}$ taken as a reference complex.[48] The emission spectra, rescaled according to the corresponding photoluminescence quantum yields, are illustrated in Figure 4, and data recorded in MeOH/EtOH (1:4) frozen mixtures at 77 K are displayed in Figure 5 [rhodium(III) and iridium(III) complexes, top, and ruthenium(II) derivatives, bottom, in both figures].

We first examine the behavior of the ruthenium(II) complexes, which serve as useful reference cases. The emission maxima (λ_{max}; Table 2) of the [Ru(DIP)$_2$(N^N)]$^{2+}$ derivatives **5** and **6** were red-shifted with respect to the parent

(44) Calogero, G.; Giuffrida, G.; Serroni, S.; Ricevuto, V.; Campagna, S. *Inorg. Chem.* **1995**, *34*, 541–545.
(45) Didier, P.; Ortmans, I.; Kirschdemesmaeker, A.; Watts, R. J. *Inorg. Chem.* **1993**, *32*, 5239–5245.
(46) Roundhill, D. M. *Photochemistry and Photophysics of Metal Complexes*; Plenum Press: New York, 1994.
(47) Polson, M.; Fracasso, S.; Bertolasi, V.; Ravaglia, M.; Scandola, F. *Inorg. Chem.* **2004**, *43*, 1950–1956.
(48) Juris, A.; Balzani, V.; Barigelletti, F.; Campagna, S.; Belser, P.; Vonzelewsky, A. *Coord. Chem. Rev.* **1988**, *84*, 85–277.

Table 2. Photophysical Properties for the Series of Six Ruthenium, Rhodium, and Iridium Metal Complexes, in Air-Equilibrated and Deoxygenated (Data in Parentheses) Dilute Acetonitrile Solutions

	absorption		emission (RT)			emission (77 K)	
name	λ_{max}, nm	ϵ, M^{-1} cm^{-1}	λ_{max}, nm	ϕ	τ, ns	λ_{max}, nm	τ, μs
1	259	35 100	570	0.003 (0.010)	37.5	458	>100[b]
	302	19 800					6.5
	358	5 250					
2	256	44 800	565	0.037 (0.170)	71.2	550	2.9
	320 sh	19 000					
	370 sh	8 800					
	467	1 100					
3	258	38 500	550	0.003 (0.004)	25.6	520	5.6
	308	20 600					
	364 sh	5 950					
4	258	60 700	624	0.019 (0.020)	69.5	576	1.4
	310 sh	26 900					
	370 sh	8 800					
	457 sh	2 150					
5	279	88 750	625	0.007 (0.071)	380	610	5.7
	442	20 550					
	464 sh	19 900					
6	278	74 650	642	0.013 (0.074)	262	623	3.8
	442 sh	18 850					
	466	20 250					
$[Ru(bpy)_3]^{2+}$[a]	288	76 600	615	0.015 (0.086)	170 (860)		
	452	14 600					

[a] Data from refs *Coord. Chem. Rev.* **1988**, *84*, 85, and *J. Chem. Soc., Dalton Trans.* **1995**, 3601. [b] A biexponential decay is observed, with a long-time component not exactly determined with our experimental apparatus.

$[Ru(bpy)_3]^{2+}$ complex (λ_{max} = 615 nm) and dependent on the number of carboxylic groups attached to the bpy ligand. This red shift is consistent with the withdrawing character of the −COOH substituents, which stabilizes the lowest unoccupied molecular orbital of the bpy ligand, leading to a decrease in the energy of the ^{3}MLCT level, responsible for the observed emission properties. Upon passing from room temperature to 77 K, both complexes exhibit a blue shift of the emission maxima of about 400−500 cm^{-1} (see Table 2), as expected from the ^{3}MLCT character of the emission.[2,48]

The ruthenium(II) complexes **5** and **6** are highly luminescent in oxygen-free solvent, with luminescence quantum yields $\phi \approx 0.07$, in line with the results for the parent complex $[Ru(bpy)_3]^{2+}$.[1,48] The registered oxygen-quenching effect corresponds to a 6−10-fold reduction in luminescence features with respect to degassed solutions. Luminescence lifetimes are always longer than that of the reference complex ($\tau_{Ru(bpy)_3}$ = 170 ns, in air-equilibrated acetonitrile) and decrease with an increase in the number of carboxylates attached too, according to the "energy gap law", predicting an enhancement of nonradiative transitions for lower and lower energy gaps between the emitting level and the ground state.[49] On the other hand, the emission quantum yield (ϕ; Table 2) increases with an increase in the number of carboxylic substituents and remains comparable to that of the parent complex (ϕ = 0.015), in contrast to the observed trend in luminescence lifetimes. This behavior is revealing of a more complex situation and could be explained on the basis of the well-known interplay of low-lying MLCT emitting levels and higher-lying nonemissive metal-centered (MC) levels. In fact, the heteroleptic $[Ru(DIP)_2(N^\wedge N)]^{2+}$ derivatives studied are likely to display emission properties related to very close-lying ^{3}MLCT excited states originating from both ^{3}Ru → bpy and ^{3}Ru → DIP CT transitions. On these bases, their relative energy position can conceivably be modulated by the number of σ-withdrawing −COOH groups attached and probably by their dissociation degree as well (pH dependence); see the following section for a discussion on the pH dependence of absorption and emission properties.

In the case of the $[Rh(ppy)_2(N^\wedge N)]^+$ cyclometalated derivatives **1** and **3**, an unstructured emission band was observed at room temperature, peaking at 570 and 550 nm, respectively (Table 2 and Figure 4). The emission peak shifted toward higher energy in frozen solutions at 77 K, behavior consistent with a CT character of the luminescence. However, it is remarkable that by increasing the number of carboxylic withdrawing groups on the bpy ligand (the case of **3** with respect to the case of **1**; Figure 4, top), the emission at room temperature undergoes a blue shift. This finding rules out a ^{3}MLCT (Rh → bpy) character for the luminescence, which would instead manifest as a red shift upon and increase in the the number of withdrawing groups (appended at the bpy ligand), and supports a SBLCT (σ-bond → pyridine) or an ILCT (phenyl → pyridine) character for the involved excites states. Consistent with this, the rhodium(III) complex **1** shows at 77 K a structured emission profile of LC nature, with lifetime τ > 100 μs (Table 2). For **1** and **3** at room temperature, the determined luminescence lifetime value was 37.5 and 25.6 ns, respectively, and the quantum yield remained unchanged, with radiative constant $k_r = 1.3 \times 10^5$ and 6.9×10^4 s^{-1}, respectively (Table 2; $k_r = \phi/\tau$).

Interestingly, for the rhodium(III) complex **1**, a luminescence quantum yield ϕ = 0.01 in deaerated solutions is observed, which is a remarkable performance.[25] The luminescence of the two rhodium(III) complexes seems to undergo a different quenching effect by the molecular oxygen dissolved in solution. In fact, while for the rhodium(III)

(49) Caspar, J. V.; Kober, E. M.; Sullivan, B. P.; Meyer, T. J. *J. Am. Chem. Soc.* **1982**, *104*, 630–632.

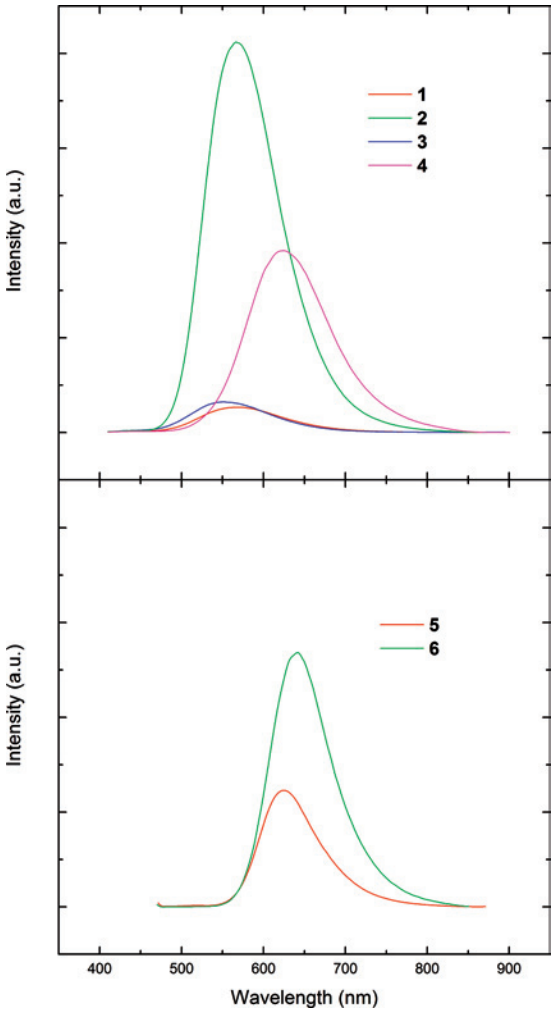

Figure 4. Luminescence spectra of the complexes at room temperature (scaled according to the photoluminescence quantum yields) recorded in a CH_3CN solvent. Top panel: $[Rh(ppy)_2(Hcmbpy)][PF_6]$ (**1**, red line), $[Ir(ppy)_2(Hcmbpy)][PF_6]$ (**2**, green line), $[Rh(ppy)_2(H_2dcbpy)][PF_6]$ (**3**, blue line), and $[Ir(ppy)_2(H_2dcbpy)][PF_6]$ (**4**, magenta line). Bottom panel: $[Ru(DIP)_2(Hcmbpy)][Cl]_2$ (**5**, red line) and $[Ru(DIP)_2(H_2dcbpy)][Cl]_2$ (**6**, green line).

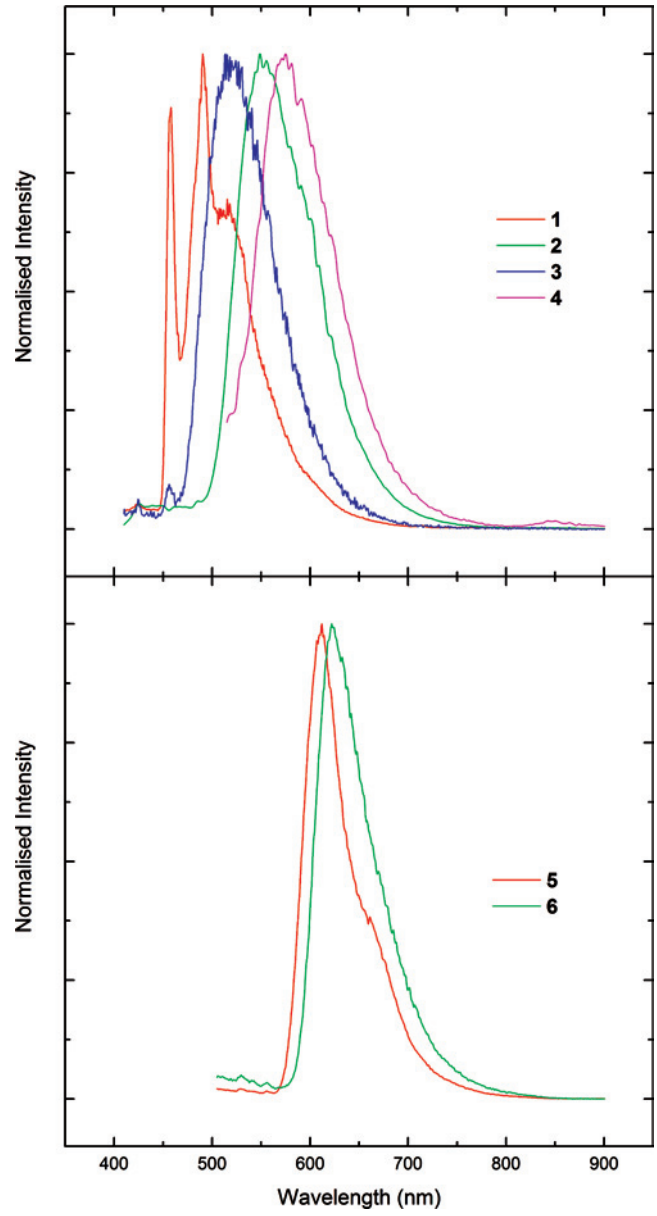

Figure 5. Luminescence spectra of the complexes recorded at 77 K in a frozen MeOH/EtOH (1:4) mixture. Top panel: $[Rh(ppy)_2(Hcmbpy)][PF_6]$ (**1**, red line), $[Ir(ppy)_2(Hcmbpy)][PF_6]$ (**2**, green line), $[Rh(ppy)_2(H_2dcbpy)][PF_6]$ (**3**, blue line), and $[Ir(ppy)_2(H_2dcbpy)][PF_6]$ (**4**, magenta line). Bottom panel: $[Ru(DIP)_2(Hcmbpy)][Cl]_2$ (**5**, red line) and $[Ru(DIP)_2(H_2dcbpy)][Cl]$ (**6**, green line).

complex **1** bearing one carboxylic group the usual enhancement of luminescence quantum yield in deaerated solutions is observed, the behavior of the rhodium(III) complex **3** with two −COOH units seems to be unaffected by the removal of dioxygen.

The $[Ir(ppy)_2(N^\wedge N)]^+$ derivatives **2** and **4** show a straightforward behavior, consistent with an ^{3}MLCT (Ir → bpy) character of the emission. Actually, the increasing number of electron-withdrawing −COOH substituents on the bpy ligand results in a red shift of the emission maximum, from 565 to 624 nm, the cases of **2** and **4**, respectively. This is accompanied by a decrease in the quantum yield and lifetime, which can simply be explained by the "energy gap law".[49] Even in this case, the same effect of the molecular oxygen on the photophysical properties previously registered for the corresponding rhodium derivatives is observed.

Dissociation of the Carboxylic Acid Groups. Titration experiments to probe the influence of the carboxylic groups on the absorption and emission spectra and lifetimes of the rhodium(III) and iridium(III) complexes **1**–**4** complexes proved not possible. Actually, in solvents different from acetonitrile, including acetonitrile/water mixtures employed in similar cases,[50] either solubility problems or degradation effects were observed.

For ruthenium(II) polypyridine complexes bearing mono- or polycarboxylate functionalities, results of titration experiments of absorption and emission spectra as performed in water are available that indicate what species are present in solution.[51,52] Thus, for the 4-carboxylic acid-4′-methyl-2,2′-bipyridine monocarboxylate species $[Ru(phen)_2(Mebpy\text{-}COOH)](PF_6)_2$, for both the ground and excited states the

(50) Guardigli, M.; Flamigni, L.; Barigelletti, F.; Richards, C. S. W.; Ward, M. D. *J. Phys. Chem.* **1996**, *100*, 10620–10628.
(51) Vos, J. G. *Polyhedron* **1992**, *11*, 2285–2299.
(52) Shimidzu, T.; Iyoda, T.; Izaki, K. *J. Phys. Chem.* **1985**, *89*, 642–645.

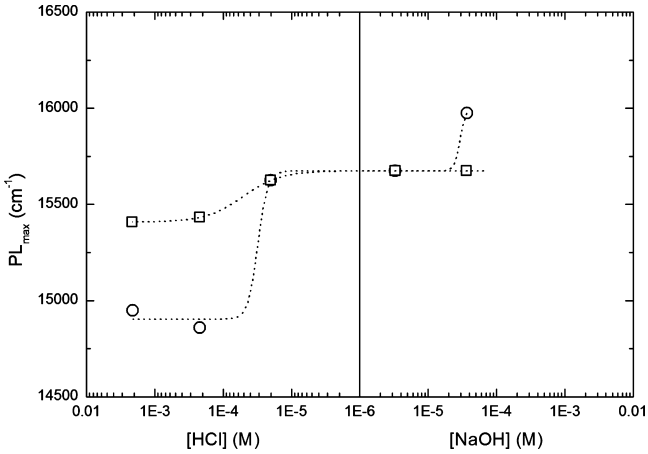

Figure 6. Comparison of the dependence of the photoluminescence band maximum of **5** (squares) and **6** (circles) acetonitrile solutions on HCl (left) and NaOH (right) concentrations.

actual cationic species present in water at pH > 5 is $[Ru(phen)_2(MebpyCOO^-)]^+$ given that the ground-state acid dissociation constant pK_a is 2.6 and that the excited-state acid dissociation constant pK_a* is 4.6.[53] The less acidic character of the excited state (i.e., the lower ability to dissociate) is a consequence of the MLCT character of the emitting level and of the fact that the involved ligand becomes more electron-rich with respect to the ground state.[51] A similar conclusion is reached for the 4,4′-dicarboxy-2,2′-bipyridine complex $[Ru(bpy(COOH)_2)_3]^{2+}$, for which only the fully 6-fold deprotonated species $[Ru(bpy(COO^-)_2)_3]^{4-}$ is found to be present at pH 7; in this complex, for the dissociation of two carboxylic acid groups, it is found that pK_a = 0.7 and pK_a* = 3.8.[54]

Figure 6 reports the changes of the luminescence band maximum as a function of HCl (left) and NaOH (right) concentration for the mono- and dicarboxylic ruthenium(II) derivatives **5** and **6**. In acidic media (Figure 6, left), both complexes show a similar behavior, with a gradual shift of the luminescence maximum to lower energy values as the H^+ concentration increases. Conversely, in basic media (Figure 6, right), no influence of the OH^- concentration on the energy of the emission is observed for the monocarboxylate derivative, while for complex **6**, a shift to higher energies appears at the highest NaOH concentration values. In this case, a plateau could not be reached, like in the acid branch of the curve, because at higher $[OH^-]$, the decomposition of the complex takes place. Thus, three luminescent species are detected, whose emission maximum is shifting to higher energy as the proton concentration decreases and the hydroxyl concentration increases. This behavior is accounted for by the presence in an acetonitrile solution of the equilibria:

$$[Ru(DIP)_2(Hcmbpy)]^{2+} \rightarrow [Ru(DIP)_2(cmbpy)]^+ + H^+$$

$$[Ru(DIP)_2(H_2dcbpy)]^{2+} \rightarrow [Ru(DIP)_2(Hdcbpy)]^+ + H^+ \rightarrow [Ru(DIP)_2(dcbpy)] + 2H^+$$

for complexes **5** and **6**, respectively. Therefore, at a proton concentration higher than 1×10^{-4} M, the undissociated doubled-charged species $[Ru(DIP)_2(Hcmbpy)]^{2+}$ and $[Ru(DIP)_2(H_2dcbpy)]^{2+}$ prevail, while the totally dissociated neutral species $[Ru(DIP)_2(dcbpy)]$ is only present at high hydroxyl concentration, with its observation being prevented by the incoming decomposition of the complex; for intermediate acid and base concentration values, the monodissociated single-charged species $[Ru(DIP)_2(cmbpy)]^+$ and $[Ru(DIP)_2(Hdcbpy)]^+$ are dominant.

For complexes **5** and **6**, the variation of the emission energy is consistent with the MLCT character of the excited states: the presence of negative charges on the bpy moiety bearing the carboxylate anion destabilizes the energy of the orbital involved in the Ru(d) → bpy(π*) transition and results in a decreased emission wavelength. A comparison of the values for the emission maximum obtained for complexes **5** and **6** at different pH values with those obtained in a pure acetonitrile solution (see Table 2) clearly shows that in the latter case the only species present is the monodissociated one.

Concluding Remarks

A series of new rhodium(III) and iridium(III) cyclometalated complexes **1**–**4** incorporating a functionalized bpy ligand with either one or two carboxylic groups were prepared and fully characterized. The structure of **2** is also reported. The photophysical properties of complexes **1**–**4** and of the related **5** and **6** species were studied. All bpy-COOH-containing ruthenium(II), rhodium(III), and iridium(III) complexes studied show luminescent properties in air-equilibrated and deoxygenated acetonitrile solutions at room temperature. The photophysical behavior of the $[Ir(ppy)_2(N^\wedge N)][PF_6]$ (**2** and **4**) and $[Ru(DIP)_2(N^\wedge N)][Cl]_2$ (**5** and **6**) derivatives can simply be accounted for by the "energy gap law" of the emitting state, a MLCT one involving the bpy ligand. For the $[Rh(ppy)_2(N^\wedge N)][PF_6]$ (**1** and **3**) derivatives, the nature of the emission level is less clear-cut and can be attributed to an ILCT level, involving the donor and acceptor moieties of the ppy ligand. Remarkably, the rhodium derivatives show a fairly intense orange luminescence in solution at room temperature ($\phi \sim 0.01$). For the complexes **1**–**4**, the energy of the emitting levels can be tuned to a large degree; for instance, λ_{max} = 565 and 624 mm for **2** and **4**, respectively, as a consequence of the number of the electron-withdrawing groups attached to the bpy ligand. The influence of the dissociation degree of the carboxylic groups on the emission properties of the ruthenium(II) derivatives has been assessed, and the species present at different pH ranges have been identified; in particular, we have shown that in a pure acetonitrile solution the only active species is the monodissociated one, which is therefore responsible for the photophysical behavior observed.

Experimental Section

All solvents used were reagent-grade or better. Deuterated solvents and commercially available reagents were used as received.

(53) Su, C. H.; Chen, H. Y.; Yun-Da, K.; Chang, I. J. *J. Phys. Chem. B* **2007**, *111*, 6857–6860.
(54) Park, J. W.; Ahn, J. H.; Lee, C. *J. Photochem. Photobiol. A: Chem.* **1995**, *86*, 89–95.

^{1}H NMR spectra were recorded on a Bruker AC-300 spectrometer. Chemical shifts are reported in ppm downfield from tetramethylsilane and are referenced to the residual hydrogen signal of deuterated solvents (CHD_2CN at 1.93 ppm and $CHDCl_2$ at 5.30 ppm). IR spectra were recorded on a Bruker Tensor 27 equipped with a Harrick ATR. Complexes **5** and **6** were prepared as reported previously by us.

[Rh(ppy)$_2$(Hcmbpy)][PF$_6$] (1). [Rh(ppy)$_2$(μ-Cl)]$_2$ (68.7 mg, 0.077 mmol) as a solution in dichloromethane (10 mL) was added via a cannula to a suspension of 4-methyl-4′-carboxy-2,2′-bipyridine (33.0 mg, 0.154 mmol) in methanol (10 mL). The reaction mixture was heated to reflux with stirring for 3 h and then cooled to room temperature. A saturated solution of ammonium hexafluorophosphate in methanol (2 mL) was added, and the mixture was stirred for a further 30 min. The volume of the solvent was then reduced to a third of the original volume under vacuum. The resulting precipitate was collected by filtration, washed with ether (2 × 5 mL), and then extracted into acetone and the solvent removed under reduced pressure. The residue was then extracted into dichloromethane and filtered to give rhodium [bis(*C*,*N*-phenylpyridine)-*N*,*N*-4-methyl-4′-carboxy-2,2′-bipyridine] hexafluorophosphate as a yellow powder (101 mg, 85%). ^{1}H NMR (500 MHz, acetone-d_6): δ 3.33 (3H, s), 6.36 (2 H, dd, J = 7.78 and 8.12 Hz, H8, H16), 6.95 (2 H, m, H7, H15), 7.05 (2 H, m, H6, H14), 7.18 (2 H, m, H2, H10), 7.46 (1 H, d, J = 5.49 Hz, H21/22), 7.75 (1 H, d, J = 5.76 Hz, H1/H9), 7.81 (1 H, d, J = 5.76 Hz, H1/H9), 7.92 (3 H, m, H21/22, H5, H13), 7.95 (2 H, m, H3, H11), 8.05 (1 H, m, H17/18), 8.22 (3 H, m, H17/18, H4, H12), 8.79 (1 H, s, H20), 9.08 (1 H, s, H19) ppm. ^{13}C NMR (125 MHz, acetone-d_6): δ 21.2, 120.9, 121.0, 124.1, 124.2, 124.3, 124.5, 125.6, 126.4, 127.8, 129.8, 130.9, 133.4, 133.5, 139.7, 143.0, 144.8, 144.9, 150.1, 150.3, 151.9, 153.4, 154.7, 156.7, 165.2, 165.7, 165.8, 168.1, 168.3 ppm. Calcd for $C_{34}H_{26}F_6N_4O_2RhP\cdot 2H_2O$: C, 50.63; H, 3.75; N, 6.95. Found: C, 50.39; H, 4.57; N, 6.76%. Mp (°C, dec): 194. IR: ν 3046 (OH), 1705 (CO), 827 (PF) cm^{-1}.

[Ir(ppy)$_2$(Hcmbpy)][PF$_6$] (2). [Ir(ppy)$_2$(μ-Cl)]$_2$ (83.0 mg, 0.077 mmol) as a suspension in methanol (10 mL) was added via a cannula to a suspension of 4-methyl-4′-carboxy-2,2′-bipyridine (33.0 mg, 0.154 mmol) in dichloromethane (10 mL). The reaction mixture was heated to reflux with stirring for 2 h and then cooled to room temperature. A saturated solution of ammonium hexafluorophosphate in methanol (2 mL) was added, and the mixture was stirred for a further 30 min. The volume of the solvent was then reduced to a third of the original volume under vacuum. The resulting precipitate was collected by filtration, washed with ether (2 × 5 mL), and then extracted into dichloromethane and the solvent removed under reduced pressure to give iridium [bis(*C*,*N*-phenylpyridine)-*N*,*N*-4-methyl-4′-carboxy-2,2′-bipyridine] hexafluorophosphate as a bright-orange powder (117 mg, 88%). ^{1}H NMR (500 MHz, CD_2Cl_2): δ 2.64 (3 H, s), 6.33 (2 H, m), 6.93 (2 H, m), 7.04 (2 H, m), 7.15 (2 H, m), 7.56 (1 H, d, J = 5.55 Hz), 7.83 (1 H, d, J = 5.55 Hz), 7.88 (3 H, m), 7.94 (3 H, m), 8.09 (1 H, m), 8.25 (3 H, m), 8.95 (1 H, s), 9.12 (1 H, s) ppm. ^{13}C NMR (125 MHz, acetone-d_6): δ 21.1, 120.6, 123.2, 124.4, 124.7, 125.7, 126.8, 128.5, 130.2, 131.1, 132.3, 132.4, 139.4, 144.7, 144.8, 149.9, 150.1, 150.6, 151.1, 152.2, 153.1, 155.9, 157.9, 168.4, 168.5 ppm. Calcd for $C_{34}H_{26}F_6N_4O_2IrP$: C, 47.50; H, 3.05; N, 6.52. Found: C, 47.16; H, 3.25; N, 6.29. Mp (°C, dec): 201. IR: ν 2963 (OH), 1721 (CO), 825 (PF) cm^{-1}.

[Rh(ppy)$_2$(H$_2$dcbpy)][PF$_6$] (3). [Rh(ppy)$_2$(μ-Cl)]$_2$ (68.7 mg, 0.077 mmol) as a solution in dichloromethane (10 mL) was added via a cannula to a suspension of 4,4′-dicarboxy-2,2′-bipyridine (37.6 mg, 0.154 mmol) in methanol (10 mL). Sodium acetate (38 mg, 0.46 mmol) in methanol (2 mL) was added, and the reaction mixture was heated to reflux with stirring for 2 h and then cooled to room temperature. A saturated solution of ammonium hexafluorophosphate in methanol (2 mL) was added, and the mixture was stirred for a further 30 min. The solvent was then removed under reduced pressure, hydrochloric acid (1 M, 10 mL) was added, and the suspension was stirred for 10 min. The product was then filtered, washed with water (2 × 10 mL), and extracted into methanol. A saturated solution of ammonium hexafluorophosphate in methanol (2 mL) was added, and the mixture was stirred for a further 30 min. The solvent was removed under reduced pressure, and the residue was extracted into dichloromethane and filtered. The solvent was removed under reduced pressure to give rhodium [bis(*C*,*N*-phenylpyridine)-*N*,*N*-4,4′-carboxy-2,2′-bipyridine] hexafluorophosphate as a yellow powder (116 mg, 94%). ^{1}H NMR (300 MHz, acetone-d_6): δ 6.38 (2 H, d, J = 7.62 Hz, H8), 7.02 (2 H, dt, J = 1.29 and 7.50 Hz), 7.13 (2 H, dt, J = 1.30 and 7.47 Hz), 7.20 (2 H, dt, J = 1.29 and 6.00 Hz), 7.88 (2 H, d, J = 5.64 Hz), 7.98 (2 H, dd, J = 1.30 and 7.77 Hz), 8.05 (2 H, dt, J = 1.44 and 6.78 Hz), 8.19 (2 H, dd, J = 1.41 and 5.40 Hz), 8.27 (2 H, d, J = 8.10 Hz), 8.36 (2 H, d, J = 5.40 Hz), 9.30 (2 H, s, H11) ppm. ^{13}C NMR (125 MHz, acetone-d_6): δ 120.9, 124.4, 124.5, 124.7, 125.6, 128.2, 130.7, 130.9, 133.3, 139.7, 142.0, 144.7, 150.2, 152.1, 156.0, 164.8, 165.6, 167.6 ppm. Calcd for $C_{34}H_{24}F_6N_4O_4RhP\cdot 2MeOH\cdot H_2O$: C, 49.89; H, 3.20; N, 6.85. Found: C, 49.65; H, 3.44; N, 6.91. Mp (°C, dec): 201. IR: ν 3046 (OH), 1705 (CO), 827 (PF) cm^{-1}.

[Ir(ppy)$_2$(H$_2$dcbpy)][PF$_6$] (4). [Ir(ppy)$_2$(μ-Cl)]$_2$ (83.0 mg, 0.077 mmol) as a solution in dichloromethane (10 mL) was added via a cannula to a suspension of 4,4′-dicarboxy-2,2′-bipyridine (37.6 mg, 0.154 mmol) in methanol (10 mL). The reaction mixture was heated to reflux with stirring for 2 h, and then sodium acetate (excess) in methanol (2 mL) was added. The mixture was heated for a further 1 h and then cooled to room temperature. A saturated solution of ammonium hexafluorophosphate in methanol (2 mL) was added, and the mixture was stirred for a further 30 min. The solvent was then removed under reduced pressure, hydrochloric acid (1 M, 10 mL) was added, and the suspension was stirred for 10 min. The product was then filtered, washed with water (2 × 10 mL), and extracted into methanol. A saturated solution of ammonium hexafluorophosphate in methanol (2 mL) was added, and the mixture was stirred for a further 30 min. The solvent was removed under reduced pressure, and the residue was extracted into dichloromethane and filtered. The solvent was removed under reduced pressure to give iridium [bis(*C*,*N*-phenylpyridine)-*N*,*N*-4,4′-carboxy-2,2′-bipyridine] hexafluorophosphate as a dark-red powder (116.7 mg, 85%). ^{1}H NMR (500 MHz, acetone-d_6): δ 6.34 (2 H, d, J = 7.50 Hz, H1), 6.94 (2 H, dt, J = 0.98 and 8.42 Hz, H2), 7.05 (2 H, t, J = 7.34 Hz, H3), 7.14 (2 H, dt, J = 0.86 and 6.16 Hz, H7), 7.90 (4 H, m, H4, H8), 7.97 (2 H, dt, J = 1.09 and 7.52 Hz, H6), 8.16 (2 H, dd, J = 1.20 and 5.53 Hz, H10), 8.24 (2 H, d, J = 8.13 Hz, H5), 8.32 (2 H, d, J = 5.58 Hz, H9), 9.33 (2 H, s, H11) ppm. ^{13}C NMR (125 MHz, acetone-d_6): δ 120.8, 123.6, 124.5, 125.5, 125.8, 129.0, 131.2, 132.2, 139.6, 141.8, 144.7, 150.3, 150.5, 152.6, 157.4, 164.8, 168.3 ppm. Mp (°C, dec): 194. IR (ATR): ν 3048 (OH), 1723 (CO), 837 (PF) cm^{-1}. Calcd for $C_{34}H_{24}F_6N_4O_4IrP$: C, 45.90; H, 2.72; N, 6.30. Found: C, 46.30; H, 3.13; N, 5.96. Mp (°C, dec): 237. IR: ν 2925 (OH), 1709 (CO), 836 (PF) cm^{-1}.

Photochemistry. UV/visible absorption spectra for acetonitrile solutions of the investigated metal complexes were measured on a Perkin-Elmer Lambda 9 UV/vis/near-IR spectrophotometer. The steady-state luminescence spectra at room temperature for air-equilibrated and argon-deoxygenated dilute (ca. 2 × 10^{-5} M) acetonitrile solutions were measured on a SPEX Fluorolog II

spectrofluorimeter, using excitation wavelengths of 450 nm for the ruthenium complex and 355 nm for the rhodium and iridium complexes, respectively. Measurements at 77 K were conducted on MeOH/EtOH (1:4) mixtures by employing quartz capillary tubes immersed in liquid nitrogen and hosted within a homemade quartz coldfinger Dewar. Luminescence quantum yields (ϕ) were evaluated at room temperature by comparing wavelength-integrated intensities (I) of the corrected emission spectra with reference to a $[Ru(bpy)_3]Cl_2$ standard ($\phi_r = 0.028$ in air-equilibrated water)[55] and by using the following equation:[56]

$$\phi_{em} = \left(\frac{In^2A_r}{AI_r n_r^2}\right)\phi_r$$

where A's are absorbance values ($A < 0.1$) at the employed excitation wavelength and n is the refractive index of the solvent. Band maxima and relative luminescence intensities were obtained with uncertainties of 2 nm and 20%, respectively. Luminescence lifetimes at room temperature and 77 K were obtained with a 5000U time-correlated single-photon-counting system (Jobin Yvon) by using a NanoLED excitation source (excitation wavelength at 465 nm for the ruthenium complex and 331 nm for the iridium and rhodium complexes). Analysis of the luminescence decay profiles against time was accomplished by using the DAS6 software provided by the manufacturer. Lifetime values were obtained with an estimated uncertainty of 10%.

X-ray Molecular Structure of 2. Suitable crystals of **2** were obtained using slow diffusion techniques from CH_2Cl_2/ether. The selected crystal was mounted onto a glass fiber and transferred in a cold nitrogen gas stream. Intensity data were collected with a Bruker Nonius-Kappa CCD with graphite-monochromated Mo Kα radiation. Unit-cell parameter determination, data collection strategy, and integration were carried out with the Nonius EVAL-14 suite of programs.[57] The structure was solved by direct methods using the *SHELXS-86* program[58] and refined anisotropically by full-matrix least-squares methods using the *SHELXL-97* software package.[59]

Acknowledgment. H.A. thanks CNRS for providing to J.B.W. a CNRS postdoctoral stipend. We thank the "Université Pierre et Marie Curie-Paris 6" and CNRS for supporting this work. This work was partially supported by the CNR Project PM.P04.010 "Materiali Avanzati per la COnversione di energia Luminosa (MACOL)".

Note Added after ASAP Publication. This article was released ASAP on March 15, 2008, with minor errors in the captions of Figures 3–5. The correct version was posted on March 20, 2008.

Supporting Information Available: X-ray crystallographic files in CIF format for the structure determination of **2**. This material is available free of charge via Internet at http://pubs.acs.org.

IC702327Z

(55) Nakamaru, K. *Bull. Chem. Soc. Jpn.* **1982**, *55*, 2697–2705.
(56) Demas, J. N.; Crosby, G. A. *J. Phys. Chem.* **1971**, *75*, 991–1024.
(57) Duisenberg, A. J. M.; Kroon-Batenburg, L. M. J.; Schreurs, A. M. M. *J. Appl. Crystallogr.* **2003**, *36*, 220–229.
(58) Sheldrick, G. M. *SHELXS-86*; University of Goettingen: Goettingen, Germany, 1986.
(59) Sheldrick, G. M. *SHELXL-97*; University of Goettingen: Goettingen, Germany, 1997.